



# Co-combustion properties of torrefied rice straw-sub-bituminous coal blend and its Hardgrove Grindability Index

Mandeep Singh<sup>1</sup> · Ashish Gupta<sup>1</sup> · Kushagra Yadav<sup>1</sup> · Karishma Jain<sup>1</sup> · Preeti Shrivastava<sup>1</sup> · R. K. Seth<sup>1</sup> · Amit Kulshreshtha<sup>2</sup> · S. R. Dhakate<sup>1</sup>

Received: 16 March 2021 / Revised: 3 June 2021 / Accepted: 22 June 2021 / Published online: 9 July 2021  
© The Author(s), under exclusive licence to Springer-Verlag GmbH Germany, part of Springer Nature 2021

## Abstract

Combustion behavior of rice straw torrefied at 300 °C for different residence time and their blends with sub-bituminous coal was investigated. The torrefied product and its blends were characterized for fuel properties and Hardgrove Grindability Index (HGI). Also, the torrefied product is characterized for density, proximate and ultimate analysis, energy yield, and structural analysis by Raman spectroscopy. The calorific value data of blend shows its value is equivalent to the value of sub-bituminous coal, i.e., 17.21 MJ/kg. On the other hand, HGI of torrefied product is 40–45 and that of coal is 80. On blending, the value of HGI up to a certain ratio shows the synergetic effect while higher content of the torrefied product in blend demonstrated non-additivity behavior and it is dominated by coal as a consequence of density difference between torrefied product and coal. Characteristic combustion parameter for blends reveals the synergetic behavior. It is found that the blend of torrefied products and sub-bituminous coal at a ratio of 10:90 and 20:80 had ignition and burnout temperature almost close to coal sample. The ignition and burnout temperature of 10:90 of torrefied product at 300 °C for 60 and 120 min are 295 °C and 507 °C, 301 °C and 505 °C whereas that of sub-bituminous coal is 325 and 515 °C. The change in the fuel properties of the blend suggests there is a certain degree of interaction that occurred during combustion.

**Keywords** Torrefaction · Rice straw · Co-combustion · Hardgrove Grindability Index · Calorific value

## 1 Introduction

The growth of any country is related to economic development which is inspired by continuous energy consumption. Most of the energy demand is fulfilled by the use of fossil fuels as energy sources as well as syngas from coal gasification as alternative fuel [41]. In the recent times, scientists are looking for alternate sources of energy, in this direction number of studies are focused on development of renewable fuels such as hydrogen [3], biofuels such as bio diesel from organic or biomass waste by supercritical and

microwave-assisted transesterification method [48], and bio-coal for thermal power plants from waste biomass [32, 38].

A country like India is satisfying most of the energy needs by generating two hundred GW of power through coal-based thermal power plants. This consumes approximately 1000 million tonnes of sub-bituminous coal annually. According to a report by Intergovernmental Panel on Climate Change (IPCC), hard coal power plants shows higher CO<sub>2</sub> emission specifically in the range 710–950 gCO<sub>2</sub>eq/kWh has compared to natural gas combined-cycle plants generating emissions in the range of 410–650 gCO<sub>2</sub>eq/kWh [9]. However, CO<sub>2</sub> arising from thermal power plants or other sources can be utilized in combination with water to form sustainable hydrocarbon fuels by electrolysis in presence of molten salts, which not only mitigate the problem of environmental pollution as well as take us a step ahead towards sustainable energy development [2].

Biomass is an environmental friendly energy source that has different advantages such as carbon neutrality, renewability, less sulfur, and huge availability within a small period (agriculture waste, municipal solid waste, and

---

Mandeep Singh and Ashish Gupta contributed equally to this paper

✉ S. R. Dhakate  
dhakate@nplindia.org

<sup>1</sup> Advanced Materials and Devices Metrology, CSIR-National Physical Laboratory, Dr. K.S. Krishnan Marg, New Delhi 110012, India

<sup>2</sup> National Thermal Power Corporation, Noida, U.P., India

forestry waste). It is possible to reduce the overall greenhouse gas emission of an existing thermal plant [11, 17] by using agricultural biomass.

However, there are inherent problems of agriculture waste biomasses compared to sub-bituminous coal fossil fuel resources, i.e., low bulk density, high moisture content, hydrophilic nature, and low calorific value, render it difficult to use on a large scale [4]. These attributes greatly impact logistics and final energy efficiency. High moisture in rice straw is one of the primary challenges, it reduces the efficiency of the process and increases fuel production costs, leads to natural decomposition resulting in loss of quality and storage issues such as off-gas emissions (Evergreen Renewables, LLC. Biomass torrefaction as a preprocessing step for thermal conversion: Reducing costs in the biomass supply chain 2009). These collective attributes make rice straw unacceptable to use as a renewable source of energy. On the other hand, the co-combustion of agriculture waste biomass with coal in the existing power plant has received a lot of attention in recent times [29, 38, 46]. Apart from the environmental benefits, the replacement of coal partially with biomass does not require large investments in a new standalone biomass plant [1]. The co-combustion can reduce the net CO<sub>2</sub> emissions from coal-based power plants besides providing effective use of biomass. The use of biomass with coal also provides a reduction in NO<sub>x</sub> and SO<sub>x</sub> emissions [30, 31]. The co-combustion is a very effective way to dispose of waste biomass. The co-combustion of coal with different lignocellulosic biomasses are reported in the literature, such as cotton stalk [31], forest residues, olive kernel and wood [22], fir wood [39], wastes from palm oil production [21], olive tree pruning [44], woody biomass [42], pine sawdust, and oat straw [23], bagasse [10], rice husk [37], etc. There are technical challenges in the co-combustion of biomass with coal in existing coal-fired power plants. The most common challenges are low energy density causing flame instabilities in the combustion chambers [24], poor grindability resulting in higher grinding energy requirements, slagging and fouling problems in boilers [40], low biomass flowability and fluidization properties [19] leading to difficulties in feeding biomass into combustors. These facts create difficulties for utilization of biomass directly. In order to reduce these inherent problems of biomass, it requires some form of pre-treatment, pre-treatment helps to alter biomass physical and chemical properties. Among the different techniques, torrefaction is simple process. Torrefaction is a slow pyrolysis process carried out at low temperatures, within a temperature range of 200–300 °C for a different isothermal time in protective atmosphere [20]. The torrefaction process is cost-effective over to other process [11, 17], increases the calorific value and shelf life of biomass because it covert hydrophilic to

hydrophobic through destruction of -OH groups and hence biomass loses its capability of hydrogen bonding [13].

India is an agriculture-based country and it generates a lot of waste biomass from different sources. To dispose of it, generally, it is burned in the field as well as in forest land which creates a lot of environmental and socio-economic problems to humanity. The torrefaction of biomass can not only solve the problem of open field burning but also can be utilized in the production of power in co-firing with coal in the thermal power plants. During torrefaction, properties of biomass change, and the resultant darker fuel possess higher calorific value, reduced volatile content, improved hydrophobicity, and grindability, which make it suitable for co-combustion [33, 34, 45]. Also, the torrefied biomass cofired with lignite coal provides a synergistic effect in burning performance [37].

Therefore, in the present work, torrefaction of rice straw was carried out in a rotating reactor at 300 °C for different residence times and extensively studied for fuel properties in co-combustion with coal. The fuel properties as well as hard groove grindability index of different torrefied biomass samples and sub-bituminous coal blend are reported in the present work. The investigation reveals that the torrefaction at 300 °C with 120 min residence time in a rotating reactor is very much compatible for co-firing with sub-bituminous coal in the thermal power plant.

## 2 Materials and methods

### 2.1 Experimental

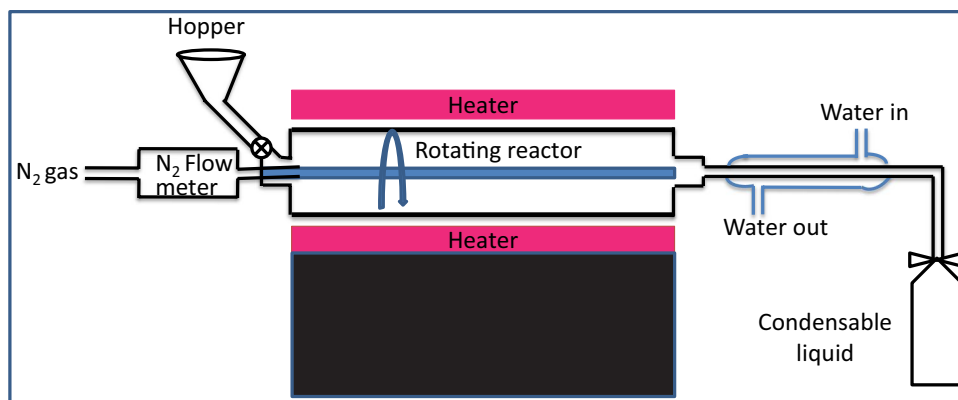
In the present investigation, the rice straw torrefaction was carried out in a laboratory-scale rotating reactor (Fig. 1) at temperature 300 °C for residence time 60, 90, and 120 min. The samples are termed RS-300–60, RS-300–90, and RS-300–120 respectively in the whole manuscript. The rotating reactor consists of a feeder, a rotary reactor unit heated by external electric heating (Fig. 1). It is controlled by a PID controller with a temperature indicator in which the thermocouple monitors the temperature in the middle of the furnace. The volatile released during the heating of biomass was condensed through a water-cooled condenser as shown in Fig. 1. Nitrogen gas was used as the carrier gas with a flow rate of 100 ml/min.

### 2.2 Characterizations

#### 2.2.1 Proximate and ultimate analysis

The TGA of the samples was carried out in the temperature range of 40–1000 °C @ 10°C/min in a nitrogen atmosphere. From the TG data, the proximate analysis was carried out

**Fig. 1** Laboratory-scale rotating type torrefaction set-up



in accordance with the standard ASTM E870-82 procedure [5]. The density of the torrefied product was measured using a specific gravity bottle of constant volume.

**2.2.2 Structural analysis**

The Raman spectroscopy is very suitable for obtaining information about the chemical structures of bio-coal. The Raman spectral measurement of torrefied rice straw and coal was carried out using Renishaw in-via Raman microscope using a laser of excitation wavelength 514 nm. The Raman spectra are deconvoluted using Voigt line shape to obtain different components.

**2.2.3 Grindability index**

Hardgrove grindability index (HGI) is determined empirically using a sample mill, according to the following procedure. The device to measure the hardgrove grindability consists of a top rotating ring with eight balls of 1 in. (25.4 mm) diameter. The ASTM standard D409 is for the measurement of HGI for coal of which bulk density is greater than 1.2 g/cc. However, the agriculture waste biomass is voluminous and low-density material (bulk density varied from 0.01 g/cc to 0.2 g/cc). After torrefaction, there is an improvement in the physical properties but not it is comparable to coal. Therefore, in this study, as per ASTM D409, it has to take 50 gm of material for measuring HGI. But due to low density, the biomass, and torrefied product were taken only 10 gm in a hardgrove testing machine sample container. The torrefied biomass was first ground with a grinder and then the material underwent a sieving process to produce a 630–1250 μm fraction of biomass. The next 10 g of the sample was inserted evenly into the hard grove testing machine. After the sample was crushed for 60 rotations by the apparatus, it was then sieved with a 75-μm sieve for 10 min. The two different fractions of biomass were then weighed using a balance.

The mass ( $m_2$ ) was the fraction of biomass that was sieved through 75 μm sieve that can be calculated using equation

$$m_2 = 10 - m_1$$

(where  $m_1$  is the biomass that was collected from 75 μm sieve).

**2.2.4 Fuel properties**

The calorific value was calculated by combustion of a unit quantity of torrefied rice straw as well as sub-bituminous coal and torrefied product blend under specified conditions [8].

The mass yield ( $M_y$ ) and energy yield ( $E_y$ ) calculated from relation (Eqs. 1 and 2) described by Bridgeman et al. [8].

$$M_y(\%) = \frac{M_{Torr}}{M_{raw}} \times 100 \tag{1}$$

where  $M_{torr}$  is Mass of torrefied product and  $M_{raw}$  is mass of raw biomass taken

$$E_y(\%) = M_y \times \frac{C_{torr}}{C_{raw}} \tag{2}$$

where  $C_{torr}$  is Calorific value of torrefied product and  $C_{raw}$  is Calorific value of raw biomass taken.

To know the fuel properties and reactivity of torrefied products as well as sub-bituminous coal and their blend, TGA studies were carried out at the heating rate 10°C/min up to 1000°C in air environment with a flow rate of air 100 ml/min.

The ignition and combustion performance of torrefied biomass was calculated from the following equations [43].

$$S = \frac{R_{max} \times R_a}{T_i^2 \times T_b}$$

where  $S$  is combustion index,  $R_{\max}$  is maximum combustion rate and it is also called DTG<sub>max</sub>,  $R_a$  is average mass loss rate it is also called DTG<sub>mean</sub>,  $T_i$  is the mean value of mass loss rate,  $T_i$  is ignition temperature, and  $T_b$  is the burnout temperature.

In the present investigation, ignition and burnout temperature was calculated by the intersection method [26]. The ignition temperature was calculated from the first DTG which crosses the TGA curve, the point at which devolatilization begins. The burnout temperature was determined from the second DTG peak. It is the position of the TGA curve at which a vertical line from the second peak of the DTG curve crosses the TGA curve. The temperature corresponding to the intersect point of tangent drawn on TGA curve and horizontal of DTG curve where stable weight loss was registered.

The activation energy of rice straw biomass, torrefied product, and blend of torrefied products-sub-bituminous coal was calculated using the Coats-Redfern method [18]. The TGA data was plotted as  $\ln\left(\frac{-\ln(1-x)}{T^2}\right)$  vs.  $1/T$  and activation energy was calculated using the following equation [7].

$$\ln\left(\frac{-\ln(1-x)}{T^2}\right) = \ln\left(\frac{AR}{HE}\left[1 - \left(\frac{2RT}{E}\right)\right]\right) - \frac{E}{RT}$$

where  $E$ (kJ/mol) is the activation energy that can be calculated from the slope of the linear fitted curve.  $R$  is the universal gas constant(8.314 J/K.mol),  $T$  is the temperature (K),  $H$  is the heating rate (°C/min), and  $A$  is the frequency factor (per min),  $x$  is a fraction of sample at time  $t$ .

### 3 Results and discussion

#### 3.1 Proximate and ultimate analysis

The bulk density of as such rice straw is very low, i.e., in the range of 0.01 g/cc because it is porous and voluminous. On the other hand, when it ground into powder its density increases to 0.22 g/cc. On torrefaction the rice straw losses more oxygen and hydrogen than carbon and as a result, there is an increase in bulk density. The bulk density after

torrefaction at 300 °C at residence time 60, 90, and 120 min, bulk density of torrefied ground powder increase to 0.37, 0.40, and 0.43 g/cc respectively. While sub-bituminous coal is used in the thermal plant having a bulk density of 0.90 g/cc which is more than double the value of the torrefied product. With increasing the residence time at 300 °C, there is a continuous release of volatile content, increases the carbon content, and as a result increase in bulk density. The torrefaction increases the density of torrefied products, which may reduce transportation costs as well as solve the storage problem. The proximate analysis calculated from the TGA data and ultimate analysis measured by elemental analyzer is illustrated in Table 1. It is observed that the moisture and volatile content decreases with increasing the residence time at torrefaction temperature 300 °C. Initially, the rice straw used possesses 6.33% moisture content, 72.67% volatile content, and 20% fixed carbon. The fixed carbon content increases from 21 to 47% for residence time 120 min at temperature 300 °C. The ultimate analysis reveals that neat rice straw consists of 38% carbon and 54% oxygen and on torrefaction carbon content increases, and hydrogen content decrease. The maximum carbon content 53.65% and oxygen content 40% in the case of sample torrefied at 300 °C for residence time 120 min. On the other hand, the sub-bituminous coal used in thermal power plants for the generation of electricity possesses a carbon content of 42% and oxygen content is 52% (Table 1). During torrefaction, dehydration and decomposition of cellulose, hemicellulose and lignin takes place in the temperature range of 200–300 °C, as a result release of gaseous products CO<sub>2</sub>, CO, small amounts of H<sub>2</sub> and CH<sub>4</sub>, which attributes in to increase in carbon content and decreases in hydrogen and oxygen. [15, 16]

Figure 2 shows the digital images of torrefied rice straw at temperature 300 °C for different residence times. As such rice straw is yellowish buton torrefaction its color changes from light brown to dark brown to blackish (Fig. 2). The color change of the rice straw is a good means of describing the degree of torrefaction. With increasing torrefaction residence time at temperature 300 °C, destructive drying is taking place, as a result, there are carbonization and devolatilization. This temperature represents the torrefaction processes limit and as a consequence disruption of most

**Table 1** Proximate and ultimate analysis of torrefied rice straw (RS)

Sample	Moisture content %	Volatile matter %	Fixed carbon %	Nitrogen wt %	Carbon wt %	Hydrogen wt %	Oxygen wt %
Neat RS	6.33	72.67	21	1.157	38.916	5.541	54.386
Coal	3.44	63.74	32.82	1.954	42.98	2.73	52.33
RS-300-60	5.84	52.36	41.8	1.815	46.726	4.289	47.349
RS-300-90	4.80	50.17	45.03	1.667	47.493	4.142	46.698
RS-300-120	3.84	48.94	47.22	1.692	53.658	4.372	40.278

**Fig. 2** Digital images of (a) as such rice straw and (b, c, d) rice straw torrefied at temperature 300 °C for different residence times of (b) 60, (c) 90, and (d) 120 min



inter-and intermolecular hydrogen bonds, C–C and C–O bonds. The cell structure of rice straw is destroyed, loses its fibrous nature, and becomes brittle. The torrefied product's color changes from dark brown to blackish, which can be mainly attributed to chemical compositional changes.

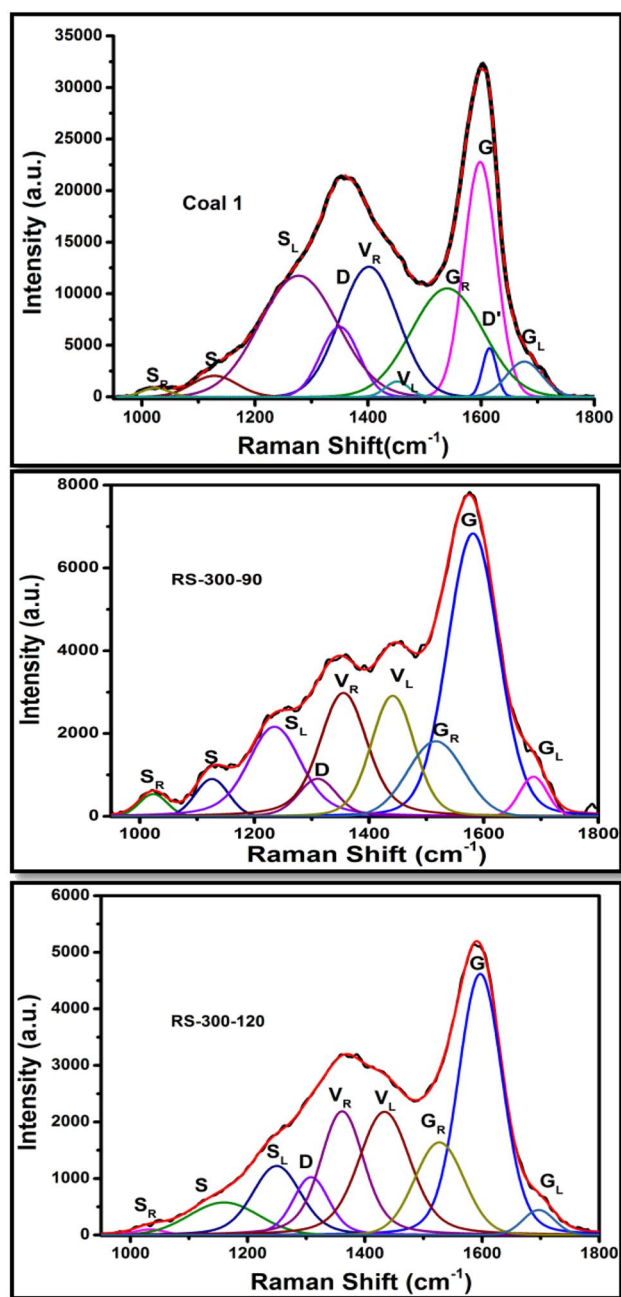
### 3.2 Structural analysis

Figure 3 shows the typical Raman spectra of sub-bituminous coal and biocoal (RS-300–90 and RS-300–120). Due to the low transmission efficiency of the light used in the spectrometer, a strong fluorescence interference as evidenced by a sloping background with the Raman shift is observed due to the insulating behavior of torrefied rice straw. To avoid the interference from the background, it is subtracted using the baseline method. The background-subtracted Raman spectra are depicted in Fig. 3. In all three samples majorly registered D and G peak at Raman shift around 1350 and 1600  $\text{cm}^{-1}$ . The spectrum was deconvoluted using the Voigt line (G+L) profile to trace out different components present in the samples. The spectrum shows the presence of peak position peak area and peak intensity summarized for the individual peak in Table 2. The peak position named SR, S,  $S_L$ , D,  $V_R$ ,  $V_L$ ,  $G_R$ , G, and  $G_L$  for peak positions near 1030, 1150, 1240, 1310, 1360, 1430, 1520, 1590, 1690  $\text{cm}^{-1}$ . The G band represents the graphite-like structure and the D band represents the defects in the carbon structure. The S-band represents the crosslinking structures and the presence of substitutional groups.  $I_S/I_G$  ratio decreases (0.13 to 0.12) with an increase

in residence time at torrefaction temperature, indicates the cross-linking and substitutional groups are removed in the increased residence time and it is nearer to  $I_S/I_G$  value in coal (0.10). These results can on the basis of destroying the disordered carbon microstructure and promoted the formation of crystalline-like carbon microstructure by poly-condensation [25]. The  $I_D/I_G$  ratio represents the defect level in the sample. As increasing the biomass torrefaction time from 90 to 120 at 300 °C, the  $I_D/I_G$  ratio increases from 0.13 to 0.22 showing an increase in defect level due to the removal of volatile matter. In the case of the coal sample, it is found highest as 0.25. However, overall graphitic character (calculated from  $I_G/I_{\text{all}}$ ) is found almost the same for coal, RS-300–90 and RS-300–120. Also, peak at 1532  $\text{cm}^{-1}$  ( $G_R$ ) arises due to the presence of amorphous carbon character in the sample, it can be seen from the table that intensity, as well as the peak area of GR band, is decreases as heat treatment time increases from 90 to 120 min and found least in the case of the coal sample. The sharpness of the G band signifies the more crystalline structure which can be observed as decreasing FWHM value with heat treatment time from 105.04 to 88.25 almost near to coal (74.57). This shows an overall increase graphitic nature of the coal sample for RS-300–120.

### 3.3 Calorific value (CV)

The calorific value is the most important fuel property of torrefied products when it will be used as a renewable source of energy instead of fossil fuel in different applications. The



**Fig. 3** Raman spectra of sub-bituminous coal and biocoal, i.e., RS-300–90 and RS-300–120. Where SR (C–H on aromatic rings; benzene (ortho-di-substituted) ring) S (Caromatic–C alkyl; aromatic (aliphatic) ethers) D (Highly ordered carbonaceous materials) VR (semi-circle breathing of aromatic rings), VL (methyl), GR (3–5 rings), G (graphitic), D' (disorder in structural organization), GL (C=O)

calorific value of the as such rice straw is in the range of 15.23 MJ/kg and after torrefaction at 300 °C for residence time 60 min, the calorific value increases to 18.21 MJ/kg, so there is around 19% enhancement in the calorific value. On further increasing the residence time at 300 °C, the calorific

**Table 2** Structural parameter calculated from Raman spectra

	SR (C–H on aromatic rings; benzene (ortho-di-substi- tuted) ring)	S (Caromatic–Calkyl; aromatic (aliphatic) ethers)	SL (Aryl–alkyl ether; para- aromatics)	D (Highly ordered carbonaceous materials)	VR (semi-circle breath- ing of aromatic rings)	VL (methyl)	GR (3–5 rings)	G	D'	GL(C=O)
COAL	1022.60	1144.28	1252.65	1326.40	1361.45	1429.77	1528.17	1595.21	1614.24	1676.16
INTENSITY	829.53	2998.43	9186.40	7400.28	7233.97	14,229.57	4288.78	28,738.4	5159.94	3948.33
AREA	0.57	4.29	13.26	9.23	7.45	28.71	3.27	27.45	1.98	3.74
FWHM	54.28	111.74	112.76	95.91	80.43	157.56	59.63	74.57	30.09	73.98
RS-300–120	1033.15	1159.69	1249.57	1308.10	1361.31	1433.53	1527.10	1596.91	1696.64	1696.64
INTENSITY	100.86	576.92	1222.64	1024.64	2187.83	2178.68	1637.98	4618.26	443.44	443.44
AREA	0.43	5.65	9.42	5.89	15.63	18.30	11.76	30.84	2.04	2.04
FWHM	60.25	139.59	97.37	72.36	87.31	104.33	99.33	88.25	63.27	63.27
RS-300–90	1023.41	1125.84	1234.96	1310.10	1355.23	1441.25	1516.44	1581.29	1686.67	1686.67
INTENSITY	539.11	902.38	2164.13	908.65	2979.99	2911.67	1812.87	6830.89	956.69	956.69
AREA	1.47	2.93	13.19	3.81	16.31	13.25	10.04	36.36	2.60	2.60
FWHM	57.15	68.01	109.35	78.47	97.91	88.71	115.13	105.04	56.87	56.87

value enhanced by 22 and 26% for the residence time 90 and 120 min. This enhancement is due to the removal of volatile products and an increase in carbon content. On the other hand, sub-bituminous coal used as an energy source in the thermal power plant has possessed the calorific value of 17.21 MJ/kg which is 14% higher than rice straw. The torrefied rice straw product has 5, 8.5, and 10.5% higher than that of sub-bituminous coal. On the other hand, on blending of sub-bituminous coal with torrefied rice straw in the ratio of 90:10, 80:20, and 70:30, it is found that the calorific value does not change significantly than the sub-bituminous coal, i.e., 17.21 MJ/kg (Table 3). In all different blend ratios, the calorific value is almost same. This suggests that biomass blending with coal does not influence the calorific value of sub-bituminous coal.

### 3.4 Grindability analysis

Grindability is an important characteristic property of the brittle raw materials for designing the mills. The grindability depends on many unknown factors and HGI is important for the up-gradation of biomass for the post-application. The HGI test is most commonly used to estimate the energy usage, capacity, and performance of the mill and the particle distribution after the milling process [12]. As a general rule, higher HGI values indicate that the fuel is easier to grind, requiring lower power inputs and giving higher mill output. The understanding of the grindability properties of the torrefied rice straw are important for their application. After torrefaction, the cell-wall structures are ruptures and develop bigger pores, elucidating the significant collapse of the cell walls [15,

16]. This is attributed to the release of volatile matter in the form of gases and condensation liquid during torrefaction [35]. Once the cell walls of biomass are destroyed, it is easier to grind the torrefied biomass, thereby improving the grindability. This improvement in grindability is crucial for fuel application. Specifically, the better grindability of material is conducive to saving more energy if the biomass is pulverized into small particles [28]. The HGI value of torrefied rice straw and its blend with sub-bituminous coal is reported in Table 4. The raw rice straw possesses a very low value of HGI in the range of 10–14 because it depends upon moisture content retain in the biomass. After torrefaction at 300 °C for different residence times, it is observed that the HGI is continuously increasing. After torrefaction, HGI is almost double and further increases up to 47 for residence time 120 min at 300 °C. However, the sub-bituminous coal is used in the thermal power plant possesses an HGI value in the range of 80–82. It has been proposed to use the torrefied rice straw in the thermal power plant with sub-bituminous coal in the different ratios in an existing plant. Therefore, it is necessary to know the value of HGI when it is used in co-firing. Table 3 also shows the HGI of sub-bituminous coal and torrefied rice straw blend. The case of torrefied product at 300 °C for residence time 120 min is taken in three different ratios demonstrating that at 10% addition of a torrefied product in sub-bituminous coal, the HGI value is in the range of 66–68 which is lower than coal and higher than a torrefied product. On the other hand, further increasing the torrefied product 20 and 30%, the value of HGI is increasing instead of decreasing. This can be due to the fact that higher content of torrefied product of lower density than bituminous coal, occupies the maximum volume in the grinding jar. The higher density of coal is settled in the downstate of the jar and the

**Table 3** Calorific value of torrefied product and its blend with sub-bituminous coal

Sample name	Calorific value (MJ/kg)
RS neat	15.23
RS-300–60 min	18.01
RS-300–90 min	18.65
RS-300–120 min	18.95
Sub-bituminous coal	17.21
Coal: RS 300–60-(90:10)	17.36
Coal: RS 300–60-(80:20)	17.15
Coal: RS 300–60-(70:30)	17.15
Coal: RS 300–90-(90:10)	17.35
Coal: RS 300–90-(80:20)	17.41
Coal: RS 300–90-(70:30)	17.43
Coal: RS 300–120-(90:10)	17.55
Coal: RS 300–120-(80:20)	17.39
Coal: RS 300–120-(70:30)	17.51

**Table 4** HGI value of torrefied rice straw and its blend with sub-bituminous coal

Sample name	HGI
RS neat	13–14
RS-300–00 min	24–26
RS-300–60 min	40–43
RS-300–90 min	43–45
RS-300–120 min	45–47
Sub-bituminous coal	82–85
Coal: RS-300–60-(90:10)	60–63
Coal: RS-300–60-(80:20)	75–76
Coal: RS-300–60-(70:30)	80–82
Coal: RS-300–120-(90:10)	66–68
Coal: RS-300–120-(80:20)	82–83
Coal: RS-300–120-(70:30)	83–84

lower density torrefied product is above the coal powder. Whereas the grinding balls are at the ground state of the jar and as a result, it will grind coal powder to a higher extent as compared to the torrefied product. This is attributed to the higher value of HGI in the case of blend ratio 80:20 and similar observation is registered in case of 70:30 ratios and HGI value is equivalent to that of bituminous coal HGI value. The improved grinding performance of the torrefied product can significantly save power consumption during biomass milling.

The mass yield and energy yield calculated from Eqs. 1 and 2 described in the method section. The energy yield decreases progressively from 93 to 70% with an increased residence time at torrefaction temperature 300 °C which is calculated from the relation between mass yield and calorific value (Eq. 1). After torrefaction at 300 °C for 0 residence time, 93% of energy is retained by torrefied products. With increasing residence time at torrefaction temperature, energy yield decreases to 72% for 120 min. The mass yield of the torrefied products also decreases from 84 to 55% with an increase in the residence time

at torrefaction temperature 300 °C. There are two main causes in the decrease of mass yield of torrefied products, one is moisture loss and the other is due to thermal decomposition of lignocelluloses rice straw which forms volatile gaseous products and increase in carbon content.

### 3.5 Combustion analysis

Figure 4 shows the TGA and DTG curves of rice straw and torrefied rice straw in air environment. In the case of raw rice straw, the TG curve demonstrated initial weight loss up to 200 °C due to the released moisture content. The major de-volatilization is taking place between temperatures 200 to 475 °C; this is due to the combustion of volatile matter and combustion of biochar plus remaining lignin. Further continuous slow weight loss up to final temperature and maximum rate of volatilization is in-between temperature 200–450 °C. The DTG curve reveals three peaks at around temperatures 292, 392, and 448 °C, a major peak at temperature 292 °C it is due to the combustion of volatile matter and as a result degradation of biomass constituent hemicellulose

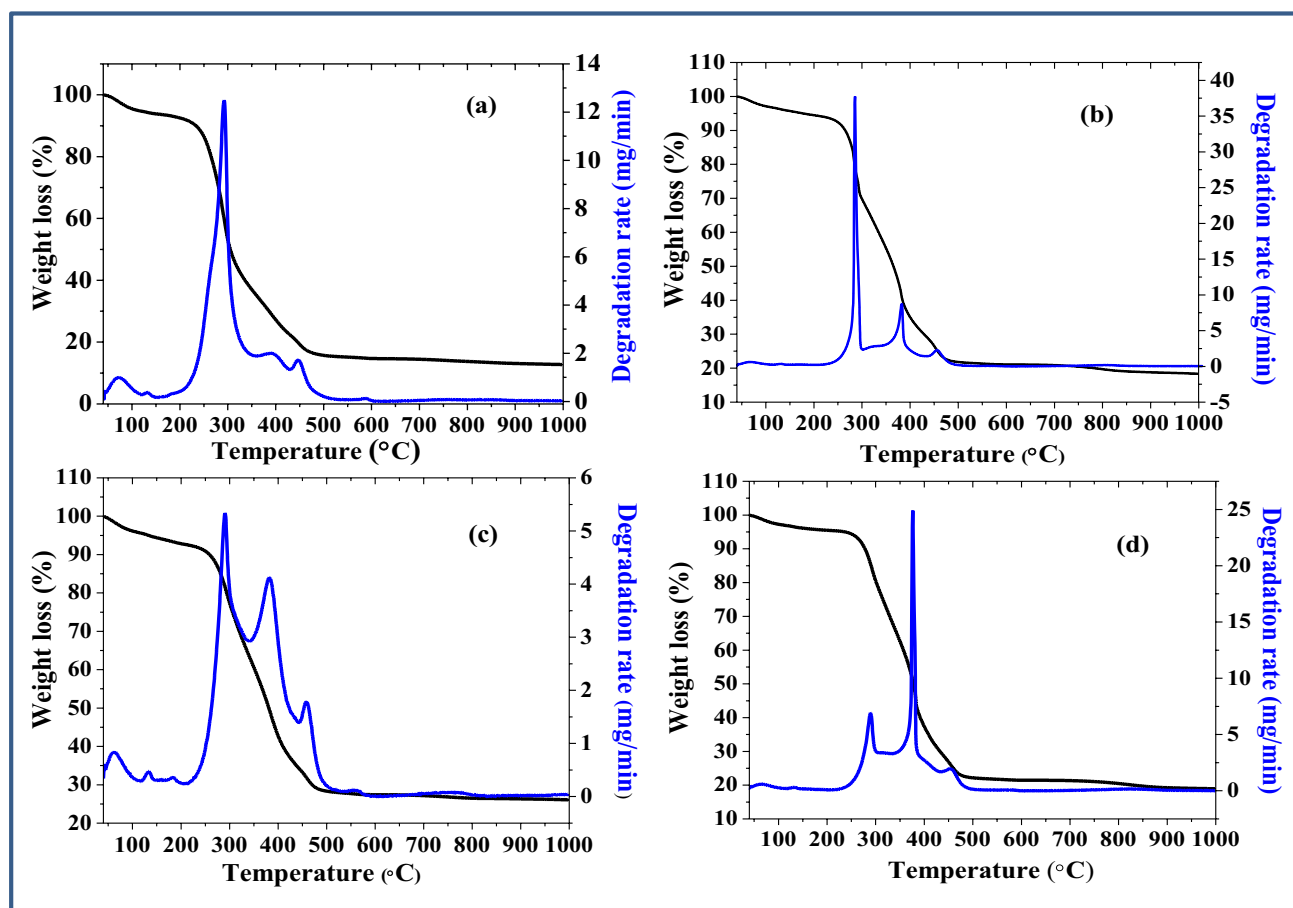


**Fig. 4** TGA rice straw (RS) curve of and torrefied rice straw carried out in oxidizing environment. (a) Neat RS, (b) RS 300–60, (c) RS 300–90, and (d) RS 300–120 (temperature(°C)–residence time(min))



and cellulose [27]. Above 300 °C, the peak observed is due to the combustion of lignin and fixed carbon in the oxidizing atmosphere [14]. After torrefaction at 300 °C, for different residence times, the peaks are sharper with higher intensity and the peak position also has redshift. After torrefaction at 300 °C for residence time 120 min, peak at temperature 376 °C is highly intense due to combustion of cellulose and at 454 °C is due to the lignin and fixed carbon combustion.

The fuel parameters are calculated from the TGA data reported in Table 3. After torrefaction, the ignition temperature increases with increasing the residence time from 60 to 120 min at temperature 300 °C. The ignition temperature of un-torrefied rice straw is 229 °C and it increases to 263 °C after torrefaction. It depends upon combustion of low molecular weight component of, e.g., volatile matter. With increasing the residence time at 300 °C, the combustion of volatile matter rate increases. On the other hand, burning temperature also increases but the extent of increase is not so high, it increases from 468 to 475 °C and it is less than the burning temperature of sub-bituminous coal. The combustion index is improved on the torrefaction of rice straw but does not show a linear relationship with residence time at 300 °C because biomass combustion is a complex reaction.

The combustion of waste biomass is a complex process because it consists of different components of different characteristics, i.e., hemicellulose, cellulose, and lignin. It is normally divided into three different reaction stages [47]. Hemicellulose consists of a complex, branched, and heterogeneous polymeric network with lower molecular weight polymers and it connects lignin and cellulose. Cellulose is along with chain polysaccharide and its structure has crystalline and amorphous parts. It consists of high molecular weight polymers of glucose that are held rigidly together fiber bundle to provide material strength [6]. On the other

hand, lignin is an amorphous polymer made by different phenolic compounds and is the main component of cell walls (tridimensional polymer and propyl-phenol that is embedded in and bound to the hemicelluloses). It provides rigidity to the structure and holds together cellulose and hemicelluloses fibers and gives support, resistance, and impermeability [36]. The TGA weight loss data is used to calculate the reaction kinetics. The activation energy is the energy required to start the reaction during the combustion process. As depicted in Fig. 4, the weight loss curve of the rice straw TG curve is divided into three steps in the liner weight loss region. The first step in the temperature range 242–306 °C, the second step 307–435 °C and in-between temperature 436–467 °C is the third step. The activation energy for the first step is 41 kJ/mol, in the second step 11, and 43 kJ/mol for the third step. After torrefaction at 300 °C for 60 min residence time, the step temperature range varies and three different steps temperature range 254–294, 294–386, and 387–462 °C and corresponding the activation energy is around 62, 19, and 17 kJ/mol. This reveals that after torrefaction the activation energy increases the first and second step; this brings out the fact that due to the release of volatile matter due to decomposition of hemicellulose and cellulose during torrefaction, during combustion process reaction higher energy is required to start the reaction. The same trend is followed with subsequent torrefaction condition of rice straw but with increasing the temperature during the combustion process third step the activation energy is lower than that of as such rice straw. This is due to the oxidation of biomass char during combustion process (Table 5).

Figure 5a shows the co-combustion TG –DTG curve of the Coal with different content of rice straw blend. In the case of combustion behavior sub-bituminous coal shows a single DTG peak centered at 447 °C. On blending of 10% of

**Table 5** Fuel properties of torrefied rice straw (RS) calculated from TGA performed in Air atmosphere up to 1000 °C

Sample Name	Ignition temp Ti (C)	Burning temp Tb (C)	R <sub>Max</sub>	R <sub>mean</sub>	Combustion Index S mg <sup>2</sup> min <sup>-2</sup> C <sup>3</sup>	Activation energy (kJ/mol)	Temp range °C
RS NEAT	229.5	468.7	0.91	12.49	4.59E-07	41.69	242–306
						11.33	307–435
						43.83	436–467
RS 300–60	257.5	470.1	0.85	37.73	10.27E-07	62.81	254–294
						19.19	294–386
						17.87	387–462
RS-300–90	256.1	482.2	0.77	5.33	1.29E-07	33.11	258–337
						29.48	337–398
						20.93	399–477
RS- 300-120	263.3	475.0	0.84	24.89	6.38E-07	60.36	264–306
						24.18	306–381
						20.32	382–464

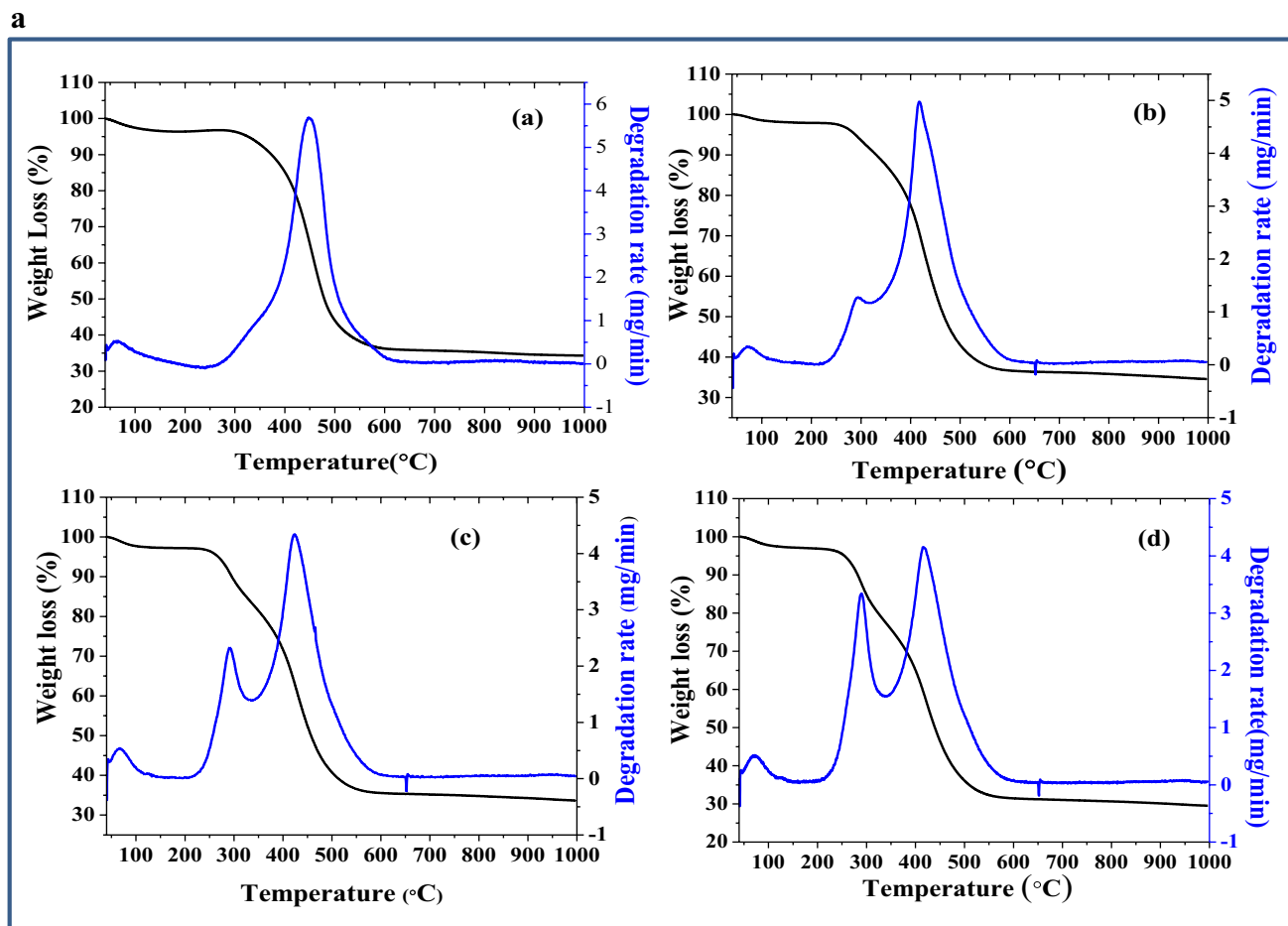


**Fig. 5** a TG-DTG curve of coal and co-combustion of RS-coal blend in different ratios (a) Coal, (b) Coal:RS ratio: 90:10, (c) Coal:RS ratio: 80:20, and (d) Coal:RS ratio: 70:30. **b** TG-DTG curve of co-combustion of torrefied RS at 300 °C for 60 min residence time-coal blend in different ratios. (a) Coal: torrefied RS ratio: 90:10, (b)

Coal:torrefied RS ratio: 80:20 and (d) Coal:torrefied RS ratio: 70:30. **c** TG-DTG curve of co-combustion of torrefied RS at 300 °C for 120 min residence time-coal blend in different ratios. (a) Coal: torrefied RS ratio: 90:10, (b) Coal:torrefied RS ratio: 80:20, and (d) Coal:torrefied RS ratio: 70:30

rice straw with coal, DTG shows two peaks one is one coal 418 °C and left shoulder peak at around 292 °C, this is due to the decomposition hemicellulose of biomass during the combustion process. With increasing the rice straw content 20 and 30% in the coal blend the shoulder peak is more prominent and it appeared at 290 and 289 °C while coal peak also shifted to lower temperature, this indicates that blending of rice straw influencing the combustion behavior of coal.

Figure 5b shows the co-combustion TG –DTG curves of the coal with different content of torrefied rice straw (300 °C for 60 min) blend. Similar to the above case, Onblending 10% of the torrefied product with coal, the DTG curve shows two peaks one is one coal 435 °C and left shoulder peak at around 317 °C, this is due to the decomposition cellulose of biomass. With increases, the torrefied content 20 and 30% in the coal blend the shoulder peak is more prominent and it appeared at ~315 °C while coal peak appeared attempt same

temperature, this indicates that blending of torrefied product influencing the combustion behavior of coal to some extent.

Figure 5c shows the co-combustion TG –DTG curves of the coal with different content of torrefied rice straw (300 °C for 120 min residence time) blend. On addition of 10% torrefied product in coal blend, DTG curve shows two peaks one is one coal 435 °C and left shoulder peak at around 334 °C, this is due to the decomposition cellulose of biomass. With increases, the torrefied content 20 and 30% in the coal blend the shoulder peak is more prominent and it appeared at ~332 °C while coal peak appeared attempt same temperature, this indicates that blending of torrefied product influencing the combustion behavior of coal to some extent. With increasing the torrefaction severity, fuel properties torrefied products approach near the properties of sub-bituminous coal and as a consequence improvement in combustion behavior properties of blends.

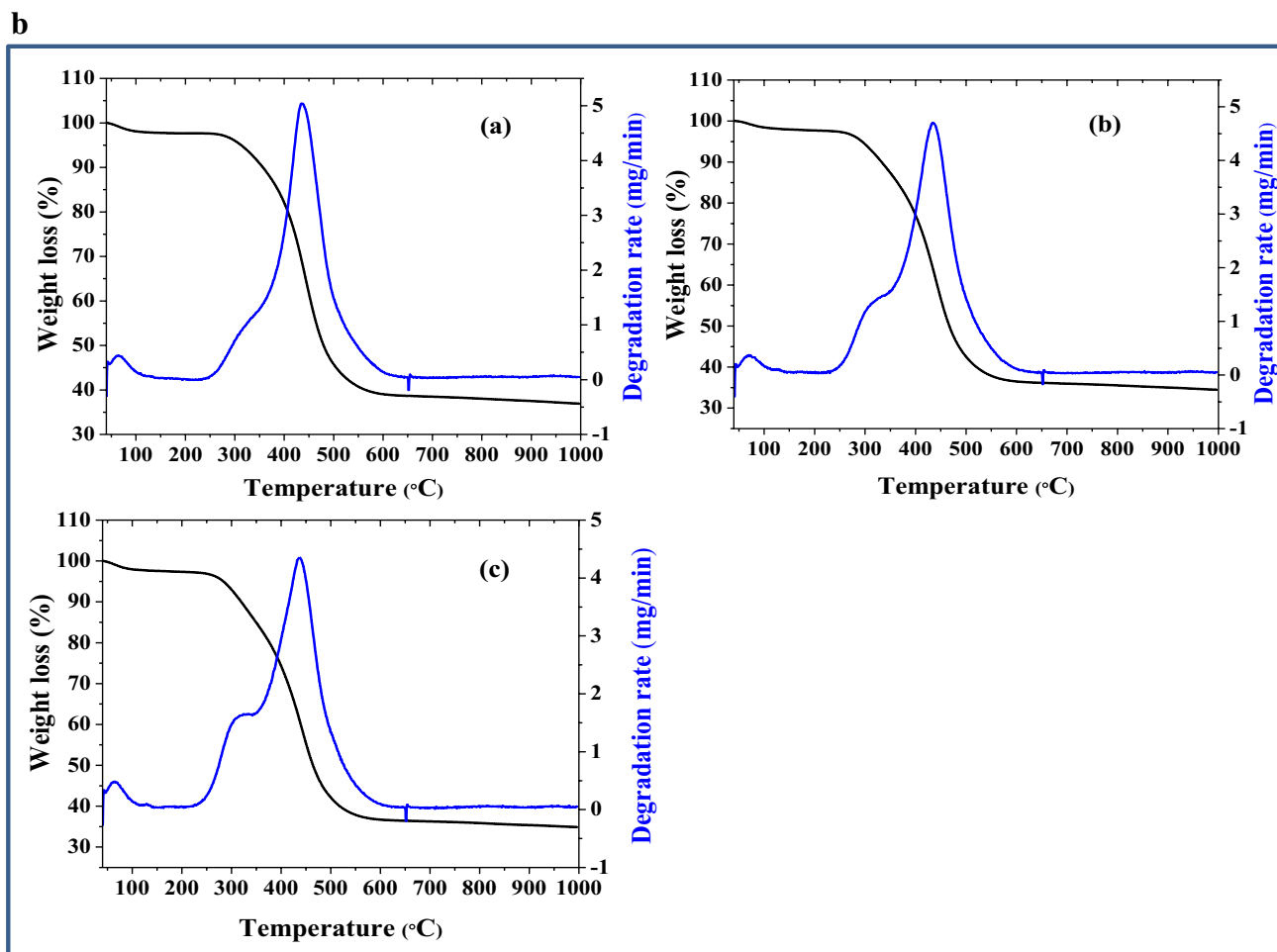


Fig. 5 (continued)

Table 6 depicted the fuel properties of coal-torrefied and un-torrefied product blends. The ignition and burning temperatures in the case of sub-bituminous coal are 325 and 515 °C. On blending with rice straw in different ratios with coal, both ignition and the burning temperature decrease with the content of rice straw and it is 246 and 493 °C for 70:30 blend ratio of coal and rice straw. With torrefaction severity, in the blend ratio, the ignition and burning temperature difference is minimizing between coal-torrefied product blend and coal.

The combustion index in the case of sub-bituminous coal is  $8.87 \times 10^{-8} \text{ mg}^2 \text{ min}^{-2} \text{ C}^{-3}$ , on blending with rice straw biomass and torrefied product combustion index increases in case of RS-coal blend with increasing RS content. While in the case of torrefied RS and coal blend, the combustion index decreases to  $7.45 \times 10^{-8} \text{ mg}^2 \text{ min}^{-2} \text{ C}^{-3}$ . In the case of torrefied RS-coal blend (torrefied rice straw at 300 °C for 120 min), the combustion index is close to the value that of coal. The higher value of combustion index in case of Coal:RS neat blend due to more oxygen content as a consequence

of neat RS oxygen content which resulted in to lower ignition and burning temperature. After torrefaction the oxygen content decreases and carbon content increases, this results in an improvement in the ignition temperature and burning temperature as reported in Table 5. On blending of coal with the torrefied product, the combustion index decreases in all three cases as compared to coal because of lower oxygen content.

The activation energy of sub-bituminous coal at a single step is 34.05 kJ/mol in a temperature range of 342–497 °C. However, in RS-coal blend activation energy is decreased in two steps but in a combination of both the step activation energy, overall it is higher; this shows that lower reactivity of blend as compared to sub-bituminous coal. In torrefied RS-coal blend activation energy increase with increasing torrefied RS content in mild torrefied products (300 °C for 60 min residence time). In case of severe torrefied product blends (300 °C for 120 min residence time), activation energy is approaching close to the activation energy of coal in ration 70:30. This brings out the fact the fuel properties

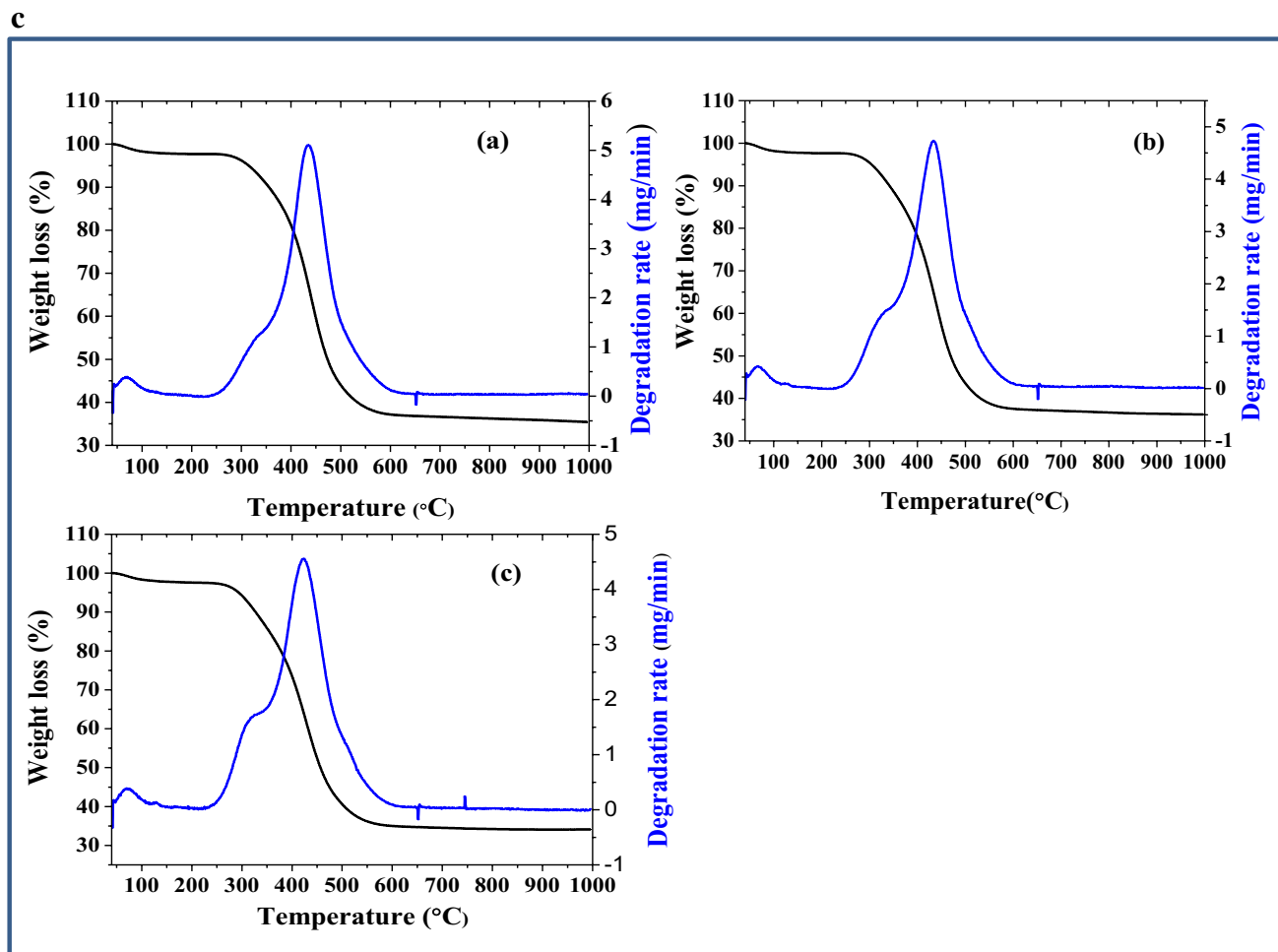


Fig. 5 (continued)

of severely torrefied product blend with coal are somewhat similar to fuel properties of sub-bituminous coal. This also in agreement with Raman spectroscopic studies of the torrefied product (300 °C for 120 min residence time), structural parameters approaches towards the coal-like properties having lower reactivity. If compared the data of torrefied rice straw and its blend with sub-bituminous coal (Table 6), it brings out the fact that change in the value of ignition and burnout temperature is due to the synergistic effect between the blending constituent.

## 4 Conclusions

In the present study, the fuel properties of the torrefied rice straw-coal blend and its HGI value demonstrated the positive judiciousness for utilization in the existing thermal power plant. The torrefaction of waste biomass rice straw is carried out successfully in a rotating reactor at 300 °C for different residence times. The co-combustion properties investigated

for RS 300–60 and RS 300–120 demonstrated that 120 min torrefied products give significantly appropriate fuel properties and HGI index. The energy yield decreases progressively from 93 to 70% with an increased residence time at torrefaction temperature 300 °C. The calorific value of blend is equivalent to that of sub-bituminous coal, i.e., 17.21 MJ/kg. The HGI value of the torrefied product (40–45) is lower than coal (80), while, on blending with coal, HGI increases up to a certain ratio shows the synergistic effect. However, higher content of the torrefied product in blend demonstrated non-synergistic behavior and it is dominated by coal as a consequence of density difference between torrefied product and coal. After torrefaction, the oxygen content decreases and carbon content increases, this results in an improvement in the ignition temperature and burning temperature. The ignition and burnout temperature of biochar: coal in the ratio 10:90 (torrefied product at 300 °C) for residual time 60 and 120 min are 295 °C and 507 °C, 301 °C and 505 °C whereas that of sub-bituminous coal is 325 and 515 °C. The change in the value of ignition and burnout temperature of

**Table 6** Fuel properties of coal blended with different proportions of raw and torrefied rice straw biomass samples

Sample name	Ignition Temp Ti (°C)	Burning temp Tb (°C)	R <sub>Max</sub>	R <sub>mean</sub>	Combustion Index (Sx10 <sup>-8</sup> ) mg <sup>2</sup> min <sup>-2</sup> C <sup>-3</sup>	Activation energy (kJ/mol)	Temp range (°C)
Bituminous Coal	325.50	515.18	0.68	7.12	8.87	34.05	342–497
RS NEAT+COAL 10:90	268.89	503.29	0.682	4.983	9.34	22.35 36.66	253–401 401–500
RS NEAT+COAL 20:80	251.87	496.15	0.690	4.344	9.52	27.98 28.27	265–363 363–483
RS NEAT+COAL 30:70	246.93	493.68	0.733	4.153	10.1	25.01 27.78	239–374 374–483
RS-300–60+COAL 10:90	295.79	507.14	0.656	5.040	7.45	29.11 42.71	307–405 404–499
RS-300–60+COAL 20:80	285.91	500.82	0.682	4.710	7.84	24.34 34.77	273–409 409–514
RS-300–60+COAL 30:70	271.36	496.83	0.670	4.352	7.94	24.20 38.89	280–405 406–488
RS-300–120+COAL 10:90	301.82	505.76	0.672	5.108	7.45	27.34 35.78	280–402 402–495
RS-300–120+COAL 20:80	287.43	498.62	0.664	4.738	7.63	26.42 45.92	281–413 413–483
RS-300–120+COAL 30:70	277.40	493.68	0.686	4.558	8.23	26.10 37.98	273–409 409–491

blend attributed to the synergistic behavior of both torrefied biomass and coalin blend. Also, the combustion index in the case of sub-bituminous coal is  $8.87 \times 10^{-8} \text{mg}^2 \text{min}^{-2} \text{C}^{-3}$ , on blending with rice straw biomass and torrefied product combustion index increases in case of RS-coal blend with increasing RS content. While in the case of torrefied RS and coal blend, the combustion index decreases to  $7.45 \times 10^{-8} \text{mg}^2 \text{min}^{-2} \text{C}^{-3}$ . The present investigation results clearly bring out the fact that utilization of torrefied product co-firing with sub-bituminous coal increase the fuel properties with synergic effect.

**Acknowledgements** The authors would like to thank Director, NPL for his constant encouragement and permission for publishing the work. The authors also thank National Thermal Power Corporation, Noida, India, for financial assistant.

## References

- Aho M, Gil A, Taipale R, Vainikka P, Vesala H (2008) A pilot scale fireside deposit study of co-firing Cynara with two coals in a fluidized bed. *Fuel* 87:58–69
- Al-Juboori O, Sher F, Khalid U, Niazi MBK, Chen GZ (2020) Electrochemical production of sustainable hydrocarbon fuels from CO<sub>2</sub> co-electrolysis in eutectic molten melts. *ACS Sustain Chem Eng* 8:12877–12890
- Al-Shara NK, Sher F, Iqbal SZ, Curnick O, Chen GZ (2021) Design and optimization of electrochemical cell potential for hydrogen gas production *Journal of Energy. Chemistry* 52:421–427
- Arias B, Pevida C, Feroso J, Plaza M, Rubiera F, Pis J (2008) Influence of torrefaction on the grindability and reactivity of woody biomass. *Fuel Process Technol* 89:169–175. <https://doi.org/10.1016/j.fuproc.2007.09.002>
- ASTM (2006) Standard Test Methods for Analysis of Wood Fuels vol E870–82. ASTM International, West Conshohocken. <https://doi.org/10.1520/E0870-82R06>
- Basu P (2018) Biomass gasification, pyrolysis and torrefaction: practical design and theory. Academic press, Cambridge, Massachusetts, United States
- Behera D, Nandi BK, Bhattacharya S (2019) Chemical properties and combustion behavior of constituent relative density fraction of a thermal coal. *Energy Sources A Recover Util Environ Effects* 41:654–664
- Bridgeman T, Jones J, Shield I, Williams P (2008) Torrefaction of reed canary grass, wheat straw and willow to enhance solid fuel qualities and combustion properties. *Fuel* 87:844–856. <https://doi.org/10.1016/j.fuel.2007.05.041>
- Bruckner T et al (2014) Energy systems, In: Edenhofer O et al (ed) *Climate Change 2014: Mitigation of Climate Change. Contribution of Working Group III to the Fifth Assessment Report of the Intergovernmental Panel on Climate Change*, Cambridge University Press, Cambridge, United Kingdom and New York, NY, USA
- Chen C, Qin S, Chen F, Lu Z, Cheng Z (2019) Co-combustion characteristics study of bagasse, coal and their blends by thermogravimetric analysis. *J Energy Inst* 92:364–369
- Chen WH, Lin BJ, Lin YY, Chu YS, Ubando AT, Show PL, Ong HC, Chang JS, Ho SH, Culaba AB, Petrisans A, Petrisans M

- (2021) Progress in biomass torrefaction: Principles, applications and challenges. *Prog Energy Combust Sci* 82:100887
12. Chen D, Zheng Z, Fu K, Zeng Z, Wang J, Lu M (2015) Torrefaction of biomass stalk and its effect on the yield and quality of pyrolysis products. *Fuel* 159:27–32. <https://doi.org/10.1016/j.fuel.2015.06.078>
  13. Chen D, Zhou J, Zhang Q, Zhu X, Lu Q (2014) Upgrading of rice husk by torrefaction and its influence on the fuel properties. *BioResources* 9:5893–5905 [https://ojs.cnr.ncsu.edu/index.php/BioRes/article/view/BioRes-09\\_4\\_5893\\_Chen\\_Rice\\_Husk\\_Torrefaction\\_Fuel](https://ojs.cnr.ncsu.edu/index.php/BioRes/article/view/BioRes-09_4_5893_Chen_Rice_Husk_Torrefaction_Fuel)
  14. Chen W-H, Kuo P-C (2010) A study on torrefaction of various biomass materials and its impact on lignocellulosic structure simulated by a thermogravimetry. *Energy* 35:2580–2586
  15. Chen W-H, Lin B-J, Colin B, Chang J-S, Pétrissans A, Bi X, Pétrissans M (2018) Hygroscopic transformation of woody biomass torrefaction for carbon storage. *Appl Energy* 231:768–776. <https://doi.org/10.1016/j.apenergy.2018.09.135>
  16. Chen D, Gao A, Cen K, Zhang J, Cao X, Ma Z (2018) Investigation of biomass torrefaction based on three major components :Hemicellulose, cellulose, and lignin. *Energy Convers Manag* 169:228–237229
  17. Chen W-H et al (2021) Progress in biomass torrefaction: Principles, applications and challenges. *Prog Energy Combust Sci* 82:100887
  18. Coats AW, Redfern J (1964) Kinetic parameters from thermogravimetric data. *Nature* 201:68–69
  19. Cui H, Grace JR (2007) Fluidization of biomass particles: A review of experimental multiphase flow aspects. *Chem Eng Sci* 62:45–55
  20. Dhakate S, et al (2019) Rice straw biomass to high energy yield bio coal by torrefaction: Indian perspective. *Curr Sci* (00113891) 116
  21. Idris SS, AbdRahman N, Ismail K (2012) Combustion characteristics of Malaysian oil palm biomass, sub-bituminous coal and their respective blends via thermogravimetric analysis (TGA). *Bioresour Technol* 123:581–591
  22. Kastanaki E, Vamvuka D (2006) A comparative reactivity and kinetic study on the combustion of coal–biomass char blends. *Fuel* 85:1186–1193
  23. Kubacki ML, Ross AB, Jones JM, Williams A (2012) Small-scale co-utilisation of coal and biomass. *Fuel* 101:84–89
  24. Li J, Yang W, Blasiak W, Ponzio A (2012) Volumetric combustion of biomass for CO<sub>2</sub> and NO<sub>x</sub> reduction in coal-fired boilers. *Fuel* 102:624–633. <https://doi.org/10.1016/j.fuel.2012.06.083>
  25. Li L, Huang Y, Zhang D, Zheng A, Zhao Z, Xia M, Li H (2018) Uncovering structure–reactivity relationships in pyrolysis and gasification of biomass with varying severity of torrefaction. *ACS Sustain Chem Eng* 6:6008–6017
  26. Lu J-J, Chen W-H (2015) Investigation on the ignition and burn-out temperatures of bamboo and sugarcane bagasse by thermogravimetric analysis. *Appl Energy* 160:49–57. <https://doi.org/10.1016/j.apenergy.2015.09.026>
  27. Luo S, Xiao B, Hu Z, Liu S, Guan Y (2009) Experimental study on oxygen-enriched combustion of biomass micro fuel. *Energy* 34:1880–1884
  28. Manouchehrinejad M, van Giesen I, Mani S (2018) Grindability of torrefied wood chips and wood pellets. *Fuel Process Technol* 182:45–55. <https://doi.org/10.1016/j.fuproc.2018.10.015>
  29. Mu L, Wang R, Zhai Z, Zhang B, Shang Y, Yin H (2021) Evaluation of thermokinetics methodology, parameters, and coke characterization of co-pyrolysis of bituminous coal with herbaceous and agricultural biomass. *Biomass Convers Biorefinery*:1–16
  30. Munir S, Nimmo W, Gibbs BM (2010) Co-combustion of agricultural residues with coal: turning waste into energy. *Energy Fuels* 24:2146–2153. <https://doi.org/10.1021/ef901503e>
  31. Munir S, Nimmo W, Gibbs B (2010) Shea meal and cotton stalk as potential fuels for co-combustion with coal. *Bioresour Technol* 101:7614–7623
  32. Negi S, Jaswal G, Dass K, Mazumder K, Elumalai S, Roy JK (2020) Torrefaction: a sustainable method for transforming of agri-wastes to high energy density solids (biocoal). *Rev Environ Sci Biotechnol* 19(2):463–488. <https://doi.org/10.1007/s11157-020-09532-2>
  33. Phanphanich M, Mani S (2011) Impact of torrefaction on the grindability and fuel characteristics of forest biomass. *Bioresour Technol* 102:1246–1253
  34. Pimchuai A, Dutta A, Basu P (2010) Torrefaction of agriculture residue to enhance combustible properties. *Energy Fuels* 24:4638–4645. <https://doi.org/10.1021/ef901168f>
  35. Ramos-Carmona S, Martínez JD, Pérez JF (2018) Torrefaction of patula pine under air conditions: A chemical and structural characterization. *Ind Crops Prod* 118:302–310. <https://doi.org/10.1016/j.indcrop.2018.03.062>
  36. Raspolli Galletti A, Antonetti C (2012) Biomass pretreatment: separation of cellulose, hemicellulose, and lignin–existing technologies and perspectives. In: Aresta M, Dibenedetto A, Dumeignil F (ed) *Biorefinery: From Biomass to Chemicals and Fuels*, 1st edn. De Gruyter, Berlin, pp 101–122. [https://doi.org/10.1515/9783110260281\\_101](https://doi.org/10.1515/9783110260281_101)
  37. Sarkar P, Sahu S, Chakraborty N, Adak A (2014) Studies on potential utilization of rice husk char in blend with lignite for cocombustion application. *J Therm Anal Calorim* 115:1573–1581
  38. Sher F, Yaqoob A, Saeed F, Zhang S, Jahan Z, Klemeš JJ (2020) Torrefied biomass fuels as a renewable alternative to coal in cofiring for power generation. *Energy* 209:118444
  39. Taş S, Yürüm Y (2012) Co-firing of biomass with coals: Part 2. Thermogravimetric kinetic analysis of co-combustion of fir (*Abies bornmulleriana*) wood with Bepazari lignite. *J Therm Anal Calorim* 107:293–298
  40. Teixeira P, Lopes H, Gulyurtlu I, Lapa N, Abelha P (2012) Evaluation of slagging and fouling tendency during biomass co-firing with coal in a fluidized bed. *Biomass Bioenergy* 39:192–203
  41. Unar IN, Soomro SA, Maitlo G, Aziz S, Mahar RB, Bhatti ZA (2019) Numerical study of coal composition effects on the performance of gasification through computational fluid dynamic. *Int J Chem Reactor Eng* 17(11):20180204
  42. Vamvuka D, Loukakou E, Avgoustidis C, Stratakis A, Pavloutidakis F, Sfakiotakis S (2019) Co-combustion characteristics of lignite/woody biomass blends. Reactivity and fusibility assessment. *Energy Sources A Recover Util Environ Effects* 41:1–15. <https://doi.org/10.1080/15567036.2019.1668885>
  43. Vamvuka D, Sfakiotakis S (2011) Combustion behaviour of biomass fuels and their blends with lignite. *Thermochim Acta* 526:192–199. <https://doi.org/10.1016/j.tca.2011.09.021>
  44. Vamvuka D, Tsamourgeli V, Galetakis M (2014) Study on catalytic combustion of biomass mixtures with poor coals. *Combust Sci Technol* 186:68–82
  45. Van der Stelt M, Gerhauser H, Kiel J, Ptasiński K (2011) Biomass upgrading by torrefaction for the production of biofuels: A review. *Biomass Bioenergy* 35:3748–3762
  46. Vasileiadou A, Zoras S, Iordanidis A (2021) Bioenergy production from olive oil mill solid wastes and their blends with lignite: thermal characterization, kinetics, thermodynamic analysis, and several scenarios for sustainable practices. *Biomass Convers Biorefinery* 11:1–14. <https://doi.org/10.1007/s13399-021-01518-6>
  47. Wang G, Zhang J, Shao J, Ren S (2014) Characterisation and model fitting kinetic analysis of coal/biomass co-combustion. *Thermochim Acta* 591:68–74
  48. Zulqarnain AM, Yusoff MHM, Nazir MH, Zahid I, Ameen M, Sher F, Floresyona D, Nursanto EB (2021) A Comprehensive

Review on Oil Extraction and Biodiesel Production Technologies. Sustainability 13(2):788

**Publisher's note** Springer Nature remains neutral with regard to jurisdictional claims in published maps and institutional affiliations.